

The Effect of SiC Powder-Mixed Dielectric Fluid on Electrical Discharge Machining Using the Taguchi Method

Patittar Nakwong

Department of Applied Science, Faculty of Science and Technology, Phranakhon si Ayutthaya Rajabhat University, Ayutthaya, Thailand
patittar.n@aru.ac.th

Apiwat Muttamara

Faculty of Engineering, Thammasat School of Engineering (TSE), Thammasat University, Khlong Luang, Phatumthani, Thailand
mapiwat@engr.tu.ac.th (corresponding author)

Received: 10 March 2026 | Revised: 7 May 2026 | Accepted: 17 May 2026

Licensed under a CC-BY 4.0 license | Copyright (c) by the authors | DOI: <https://doi.org/10.48084/etasr.18644>

ABSTRACT

This study employs the Taguchi L9 orthogonal array to evaluate the effects of Silicon Carbide (SiC) powder addition (4 g/L, 6.3 μm particle size) in die-sinking Electrical Discharge Machining (EDM) of SKD11 tool steel by using a brass electrode. Three parameters were investigated at three levels: peak current (15–24 A), Duty Factor (DF) (60–80%), and electrode servo feed rate (120–180 mm/min). The results showed that SiC Powder-Mixed EDM (PMEDM) improved the Material Removal Rate (MRR) by approximately 9.51% and increased the regression model accuracy from an adjusted R^2 of 82.28% to 91.79% compared to conventional EDM. Surface microhardness increased from 720 HV to 850 HV, while white layer thickness increased from 8.5 μm to 12.3 μm . However, Surface Roughness (SR) (Ra) deteriorated under PMEDM conditions. DF was identified as the most influential parameter affecting both MRR and SR, whereas servo feed rate showed minimal influence. The study demonstrates that SiC-PMEDM enhances machining efficiency and surface hardening, but introduces a trade-off with surface quality, providing useful guidance for parameter optimization in rough machining applications of hardened tool steels.

Keywords-Electrical Discharge Machining; Taguchi technique; SKD11 steel; Silicon Carbide powder; electrode; Powder-Mixed EDM (PMEDM); die-sinking EDM; white layer thickness

I. INTRODUCTION

Powder-mixed Electrical Discharge Machining (PMEDM) using Silicon Carbide (SiC) particles is an effective strategy employed to enhance the performance of die-sinking EDM, particularly for difficult-to-machine hardened tool steels. Adding SiC powder to the dielectric fluid improves process efficiency by facilitating multiple sparking, bridging discharge channels, and enhancing debris evacuation, leading to higher Material Removal Rate (MRR), better surface characteristics in some cases, and reduced electrode wear [1, 2].

Research has confirmed the benefits of SiC-PMEDM for hardened tool steels. Authors in [3] demonstrated significant improvements in machining performance when processing 90CrSi steel, a material with properties comparable to SKD11. Optimization of PMEDM parameters for tool steels has been widely explored using multi-criteria decision-making

techniques [4], while electrode material selection plays an important role in achieving optimal outcomes [5].

The Taguchi method has been proven highly effective for identifying influential parameters and their interactions in EDM processes. Key factors, such as pulse duration, discharge current, and powder concentration, significantly affect MRR and surface finish [6, 7]. The method's strength lies in its ability to evaluate multiple variables efficiently and determine optimal parameter combinations with minimal experimentation [3, 8]. The advantages of SiC powder over conventional dielectrics have been further highlighted. Authors in [8] reported improved surface integrity, reduced white layer thickness, lower heat flux, and enhanced fatigue life in SiC-PMEDM of AISI D2 die steel—findings directly relevant to SKD11 due to material similarities. These results are supported by additional studies demonstrating consistent benefits across various metallic alloys [8].

Empirical applications of larger Taguchi arrays (e.g., L18) have enabled detailed assessment of machining parameters, revealing that brass electrodes combined with SiC-mixed conditions often yield improvements in surface quality compared to conventional EDM [9-11]. Such optimizations not only achieve statistical robustness but also deliver substantial practical value for processing hardened steels like SKD11 [12, 13].

The Taguchi approach is particularly well-suited for simultaneous optimization of multiple responses in EDM. Authors in [14] reported on non-metallic materials, such as ZrO₂ ceramics, while hybrid Taguchi-grey relational methods have shown promise for balancing conflicting objectives when using additive powders like SiC [4, 15, 16].

Electrode material selection remains a crucial consideration in EDM performance. Authors in [17] demonstrated how different electrode compositions influence the Electrode Wear Rate (EWR) and final surface quality, while authors in [18] explored PMEDM behavior with nickel-based superalloys. Authors in [19] further illustrated the versatility of Taguchi-based optimization for MRR enhancement in non-ferrous alloys using graphite electrodes.

The literature also documents scenarios where brass outperforms copper in terms of Ra, particularly when optimizing for surface finish under certain polarity or energy conditions, or when brass's lower melting point and different crater morphology interact with the dielectric and gap dynamics to yield smoother surfaces in specific contexts. [20]

Although prior studies on SiC-PMEDM of AISI D2 and SKD11-equivalent steels have reported improvements in MRR, surface integrity, and white layer characteristics [8, 9], most of these investigations have primarily focused on powder concentration (typically 2–10 g/L), discharge current, and pulse duration, often under fixed or limited electrode motion.

In contrast, the present study introduces two key distinctions. First, it systematically investigates the influence of electrode servo/feed speed (120–180 mm/min), a parameter that has received comparatively little attention in SiC-PMEDM literature despite its direct impact on debris flushing efficiency, inter-electrode gap stability, and discharge distribution. Moreover, it adopts a Taguchi L9 orthogonal array to provide a simplified yet robust experimental framework for simultaneously evaluating conventional EDM and PMEDM under identical conditions. This approach enables a clearer attribution of performance differences specifically to the presence of SiC powder and servo dynamics.

By addressing the coupled effects of powder addition and servo feed rate on SKD11 tool steel, this study provides new insights into process stability and surface modification mechanisms.

II. MATERIALS AND METHODS

A. Work Material

EDM experiments were performed on SKD11 tool steel, a material widely used in the mold and die industry. The experiments were conducted using a CNC-EB700L (JSEDM)

with brass electrodes. Brass was selected as the electrode material due to its low cost and stable discharge characteristics, which provide satisfactory machining performance with moderate electrode wear [20]. A schematic of the setup is presented in Figure 1, while Figure 2 shows the flowchart of the systematic experimental procedure and research methodology. The workpiece material was prepared for analyzing its chemical composition. The specimens were fabricated with dimensions of 105 x 16 x 16 mm³. The elemental composition is detailed in Table I. SiC powder (average particle size ~6.3 μm, purity >98%) was mixed into the hydrocarbon-based dielectric fluid at a concentration of 4 g/L (based on the literature optimum) [8, 9]. The mixture was continuously stirred using a magnetic stirrer to ensure uniform suspension during machining.



Fig. 1. Experimental setup illustration.

B. Design of Experiments (DoE)

This experiment employed a design grounded in the Taguchi method. The L9 array specifies the variables to be investigated, comprising four factors and three levels, which relate specifically to current, Duty Factor (DF), and electrode speed. The details of the experimental design are presented in Table II. Pulse-on-time was fixed at 32 μs, and open-load voltage was maintained at 220 V. Electrode speed refers to the servo feed rate controlled by the CNC-EB700L machine (120–180 mm/min), which influences flushing efficiency and debris removal in the inter-electrode gap.

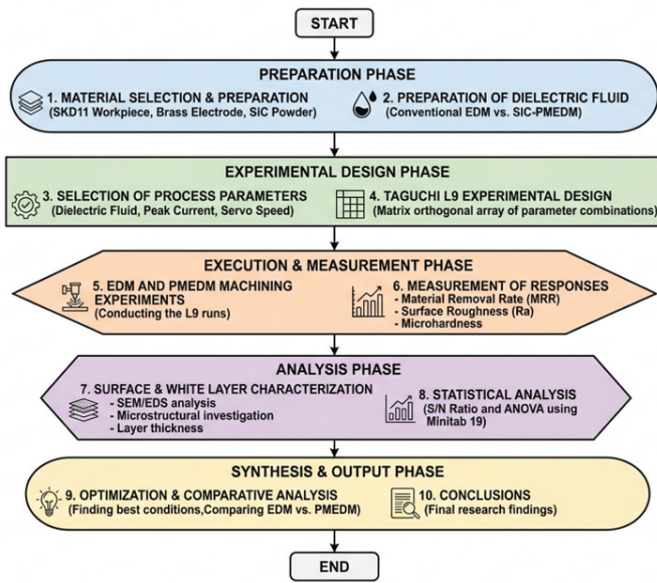


Fig. 2. Experimental research workflow.

TABLE I. ELEMENTAL COMPOSITION OF SKD11

C %	Si %	Mn %	P %	S %	Cr %	Mo %	V %	Fe %
1.40-1.60	0.6 max	0.6 max	0.03 max	0.03 max	11.0-3.0	1.0 max	1.10 max	Bal

TABLE II. INPUT PARAMETERS WITH THEIR LEVELS

Factor	Unit	Level 1	Level 2	Level 3
DF	%	60	75	80
Peak current (Ip)	A	15	20	24
Electrode speed	mm/min	120	150	180

III. RESULTS AND DISCUSSION

The experiments were systematically carried out using the Taguchi L9 orthogonal array. Each experimental condition was repeated three times, and the average values were analyzed using Minitab 19.0 through the Taguchi method and Analysis of Variance (ANOVA) to evaluate the significance of the process parameters.

For performance evaluation, the Signal-to-Noise (S/N) ratio was calculated to identify optimal conditions. The "larger-is-better" criterion (1) was applied for maximizing MRR, while the "smaller-is-better" criterion (2) was used for minimizing the Surface Roughness (SR) (Ra).

$$S/N = -10 \log_{10} (1/n \sum (1/y_i^2)) \tag{1}$$

$$S/N = -10 \log_{10} (1/n \sum y_i^2) \tag{2}$$

A. Effect of Process Parameters on MRR

The Taguchi experiment design and results are displayed in Tables III and IV. The effect of parameters on the removal rate was analyzed for both conventional EDM and PMEDM.

TABLE III. TAGUCHI EXPERIMENT DESIGN (L9)

Exp. no.	DF (%)	Ip (A)	Speed (mm/min)
1	60	15	120
2	60	20	150
3	60	24	180
4	75	15	150
5	75	20	180
6	75	24	120
7	80	15	180
8	80	20	120
9	80	24	150

TABLE IV. EXPERIMENTAL RESULTS FOR MRR AND SR

Exp. no.	MRR (mm ³ /min)		Ra (μm)	
	EDM	PMEDM	EDM	PMEDM
1	15.26	19.07	4.14	3.38
2	18.19	21.02	6.84	3.47
3	21.16	23.53	7.54	3.67
4	20.92	21.95	9.87	9.02
5	21.37	23.29	9.71	9.64
6	24.70	26.01	9.41	9.87
7	23.54	25.59	12.08	10.47
8	27.28	27.61	12.02	12.01
9	29.61	29.71	14.79	13.87

Figure 3 illustrates the main effects of process parameters on the S/N ratio for MRR in conventional EDM. The DF shows an increasing trend up to 75%, followed by a noticeable decline at 80%, indicating that excessive pulse-on time leads to unstable discharges and inefficient debris removal. The peak current (Ip) exhibits a maximum at 24 A, confirming that higher discharge energy promotes greater material removal in conventional EDM.

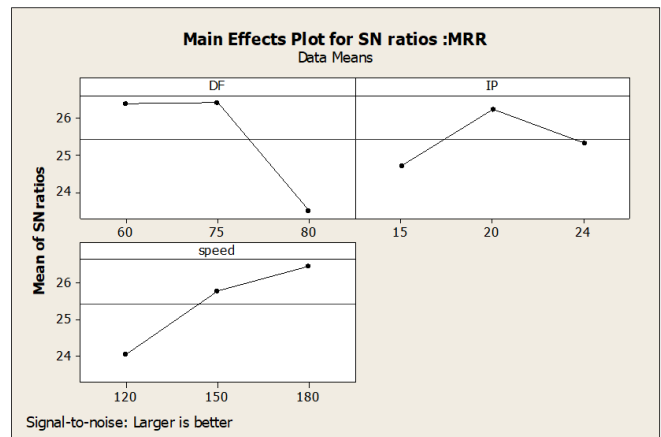


Fig. 3. Main effects influencing normal MRR on SKD11.

Similarly, cutting speed (servo/feed rate) shows a positive influence, with the highest S/N ratio at 180 mm/min, suggesting improved flushing efficiency and more stable spark generation at higher speeds. Figure 4 presents the main effects for PMEDM with SiC powder. While the DF trend remains similar, with an optimum at 75%, the behavior of peak current differs significantly. The optimal Ip shifts to a lower value of 15 A, and the S/N ratio decreases at higher currents. This indicates that, unlike conventional EDM, excessive discharge energy in PMEDM may lead to unstable plasma channels due

to the presence of suspended SiC particles. These particles reduce the breakdown strength of the dielectric and promote early spark initiation, enabling effective material removal [21, 22].

The influence of cutting speed in PMEDM is relatively less pronounced compared to conventional EDM, as indicated by the flatter slope in Figure 4. This suggests that adding SiC particles enhances debris dispersion and discharge uniformity, thereby reducing the dependency on mechanical flushing conditions. The powder particles act as conductive bridges within the spark gap, facilitating multiple discharges and distributing energy more evenly across the machining zone [23, 24].

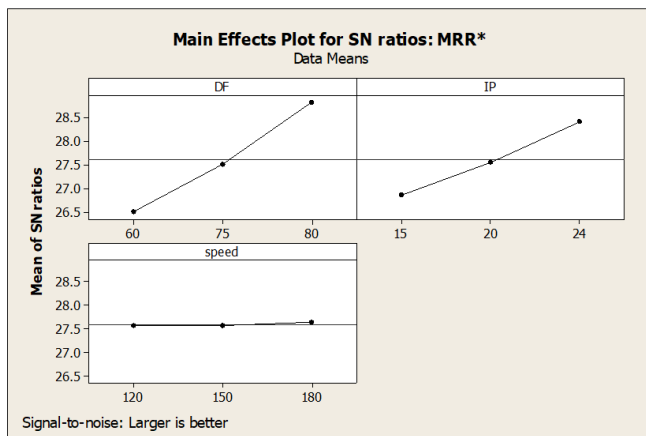


Fig. 4. Main effects on SiC powder removal rate.

The shift in optimal peak current from 24 A (conventional EDM) to 15 A (PMEDM) demonstrates the role of SiC particles in modifying the discharge mechanism. In PMEDM, the energy required to initiate and sustain sparks is reduced due to particle-assisted ionization, leading to more frequent but less intense discharges. This results in efficient material removal with lower thermal loading, which can also contribute to improved surface integrity [22].

Tables V and VI outline the ANOVA results for MRR in conventional EDM and PMEDM, respectively. The comparison confirms that PMEDM not only alters the optimal parameter settings but also changes the relative influence of machining variables. While conventional EDM relies heavily on higher discharge energy for increasing MRR, PMEDM achieves comparable or improved performance through enhanced discharge distribution and plasma channel stabilization enabled by SiC particles. These findings are consistent with previous studies reporting that powder addition allows machining at lower energy levels while maintaining or improving efficiency.

The ANOVA results indicate that the DF and peak current are the most influential parameters for both conventional and PMEDM, with high confidence levels (79.60% and 81.40% adjusted R-sq, respectively). The addition of SiC particles contributed significantly to the erosion effect. The negligible contribution of electrode speed ($P > 0.9$) indicates that within

the tested range, this parameter had minimal influence on MRR, possibly because flushing was dominated by DF and dielectric circulation rather than electrode motion.

TABLE V. ANOVA FOR NORMAL MRR

Source	DF	Seq SS	Adj MS	F-value	P-value
Regression	3	132.063	44.021	11.43	0.011
DF	1	97.619	97.619	-	0.004
Ip	1	34.440	34.440	-	0.030
Speed	1	0.004	0.004	-	0.976
Error	5	19.261	3.852		
Total	8	151.324			

TABLE VI. ANOVA FOR PMEDM MRR

Source	DF	Seq SS	Adj MS	F-value	P-value
Regression	3	79.543	26.514	12.96	0.009
DF	1	53.308	53.308	-	0.004
Ip	1	26.222	26.222	-	0.017
Speed	1	0.013	0.013	-	0.940
Error	5	10.446	2.089		
Total	8	89.989			

B. Main Effect of Process Parameters on Surface Roughness

SR is a key indicator of surface integrity, directly influenced by discharge energy, plasma channel stability, and material resolidification behavior. The main effects plots for Ra under conventional EDM and SiC-PMEDM are depicted in Figures 5 and 6, respectively. In Figure 5, the S/N ratio (smaller-is-better) improves consistently with increasing DF, indicating that higher DF (80%) leads to lower SR. Tables VII and VIII present the ANOVA results for SR in conventional EDM and PMEDM, respectively. This behavior suggests that longer pulse-on time promotes more uniform material melting and smoother crater overlapping, reducing surface irregularities. Similarly, peak current (Ip) shows a gradual improvement in Ra with increasing current, with the best condition observed at 24 A. Although higher current increases discharge energy, it also enhances crater uniformity and reduces random sparking under stable conditions [25]. The effect of cutting speed (servo/feed rate) is non-linear. The optimal condition is observed at 150 mm/min, where sufficient flushing removes debris effectively without causing discharge instability. At lower speed (120 mm/min), debris accumulation leads to secondary discharges and rougher surfaces [22, 26, 27].

In Figure 6, the overall trends are similar in terms of optimal parameter combination (DF = 80%, Ip = 24 A, Speed = 150 mm/min). However, the slopes of the curves, particularly for peak current and cutting speed, are less steep compared to conventional EDM. This indicates that the sensitivity of Ra to process parameters is reduced in PMEDM. The presence of SiC particles promotes a more uniform distribution of discharges by acting as conductive bridges within the spark gap, leading to a more homogeneous erosion process [5, 22, 23, 28, 29].

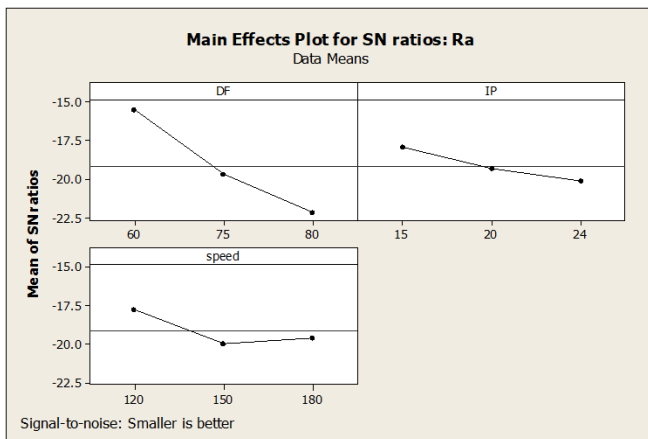


Fig. 5. Main effects plot for SR in EDM of SKD11.

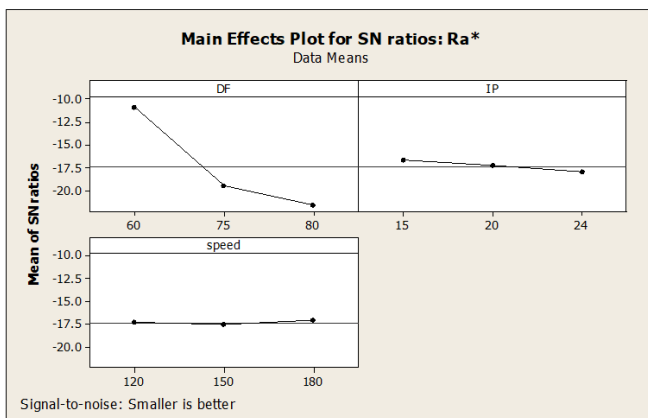


Fig. 6. Main effects plot for SR in PMEDM of SKD11.

TABLE VII. ANOVA FOR SR – CONVENTIONAL EDM

Source	DF	Seq SS	Adj MS	F-value	P-value
Regression	3	72.040	24.013	13.81	0.007
DF	1	64.443	64.443	-	0.002
Ip	1	5.251	5.251	-	0.143
Error	5	8.696	1.739		

TABLE VIII. ANOVA FOR SR – PMEDM

Source	DF	Seq SS	Adj MS	F-value	P-value
Regression	3	120.343	40.114	71.00	0.000
DF	1	116.561	116.561	-	0.000
Ip	1	3.419	3.419	-	0.057
Error	5	2.825	0.565		

Despite this stabilization effect, the average SR in PMEDM is higher than in conventional EDM. This can be attributed to several interacting mechanisms. First, the addition of SiC particles increases the frequency of random and multiple discharges, which can generate overlapping but irregular craters. Second, excessive particle concentration may reduce dielectric strength too significantly, leading to unstable plasma channel formation. Third, particle impacts and re-solidified debris can contribute to micro-protrusions on the surface.

Table IX presents the confirmation experiments conducted under the optimal machining conditions predicted by the

Taguchi analysis. The experimental results showed good agreement with the predicted values for both MRR and SR, with percentage errors ranging from approximately 4.91% to 5.54%. These relatively low deviations confirm the adequacy and reliability of the developed Taguchi models.

TABLE IX. CONFIRMATION EXPERIMENTS FOR OPTIMAL CONDITIONS OBTAINED FROM TAGUCHI ANALYSIS

Process	Optimal parameters	Predicted MRR	Experimental MRR	Error (%)
EDM	DF = 75%, Ip = 24 A, Speed = 180	MRR=0.245 mm ³ /min	MRR=0.258 mm ³ /min	5.31
PMEDM	DF = 75%, Ip = 15 A, Speed = 180	MRR=0.271 mm ³ /min	MRR=0.286 mm ³ /min	5.54
EDM	DF = 80%, Ip = 24 A, Speed = 150	Ra = 2.85 μm	Ra = 2.71 μm	4.91
PMEDM	DF = 80%, Ip = 24 A, Speed = 150	Ra = 3.12 μm	Ra = 2.95 μm	5.45

C. White Layer Characteristic Analysis

The characteristics of the white layer (recast layer) on the machined surfaces were investigated using Scanning Electron Microscopy (SEM). In conventional EDM, as shown in Figure 7, the surface exhibited typical crater morphology with a uniform distribution. In contrast, the PMEDM surface displayed more pronounced and irregular crater structures, consistent with the abrasive and conductive bridging action of SiC powder. Cross-sectional analysis revealed a thicker white layer in PMEDM specimens compared to conventional EDM, as illustrated in Figure 8.

Figure 9 presents the Vickers microhardness distribution as a function of depth from the machined surface for both conventional EDM and PMEDM. A gradient in hardness is observed in both cases, with maximum hardness at the surface that gradually decreases toward the bulk material. However, PMEDM exhibits both a higher surface hardness compared to conventional EDM.

The white (recast) layer thickness increased from 8.5 μm in conventional EDM to 12.3 μm in PMEDM, representing a 44.7% increase. This thickening is not solely due to higher spark energy, but more importantly due to modified discharge behavior in the presence of SiC particles. The suspended particles reduce dielectric breakdown strength and promote earlier discharge initiation, resulting in a wider plasma channel and more frequent secondary discharges [8]. Consequently, a larger volume of molten material is generated and re-solidified on the surface. In addition, particle-induced turbulence in the discharge gap can impair effective debris flushing, further increasing the likelihood of molten material redeposition and layer buildup.

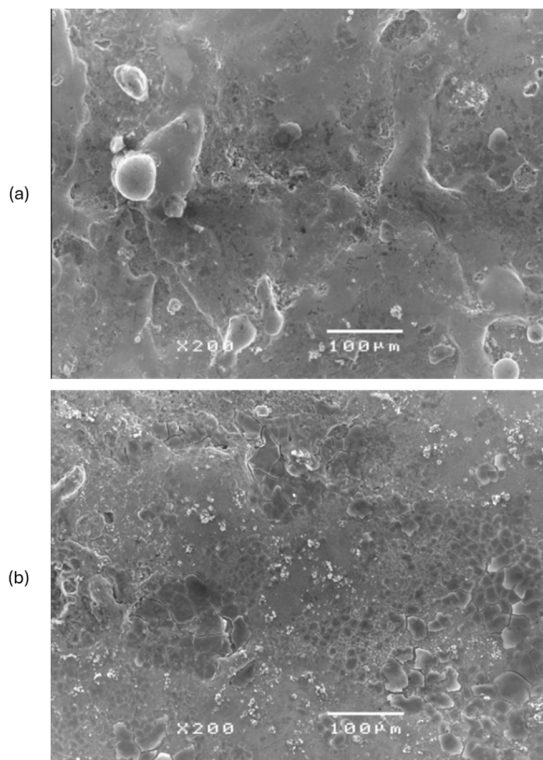


Fig. 7. SEM micrographs of the machined surfaces: (a) conventional EDM and (b) PMEDM (DF=60%, I_p =15A, Speed=120 mm/min).

At the surface, the microhardness increased from 720 HV (conventional EDM) to 850 HV (PMEDM), corresponding to an 18.1% improvement. This enhancement can be attributed to rapid quenching under high thermal gradients, which refines the microstructure and promotes the formation of metastable phases. Moreover, the presence of SiC particles contributes to carbon enrichment and carbide precipitation within the recast layer, further increasing hardness. The repeated thermal cycling in PMEDM also intensifies phase transformations, leading to a denser and harder surface layer.

A notable feature in Figure 9 is that the hardness drops sharply beyond the white layer thickness in both processes, converging to similar values in the subsurface region. This indicates that the thermal influence of both EDM and PMEDM is highly localized. Despite the increased energy input and altered discharge mechanism in PMEDM, the Heat-Affected Zone (HAZ) does not extend significantly deeper into the material. This suggests that the bulk microstructure remains largely unaffected, preserving the core mechanical properties of SKD11.

D. EDS Analysis

Energy-Dispersive X-ray Spectroscopy (EDS) was conducted to evaluate elemental composition changes on the machined surfaces. The EDS spectra are presented in Figure 10. In conventional EDM, the predominant presence of Fe (from SKD11 substrate) is observed, with minor peaks of C (from dielectric cracking) and traces from the electrode (e.g., Cu or Zn if brass was used). EDS quantification revealed that silicon content increased from ~0.5 wt% (conventional EDM)

to ~1.9 wt% (PMEDM), confirming SiC particle incorporation into the recast layer.

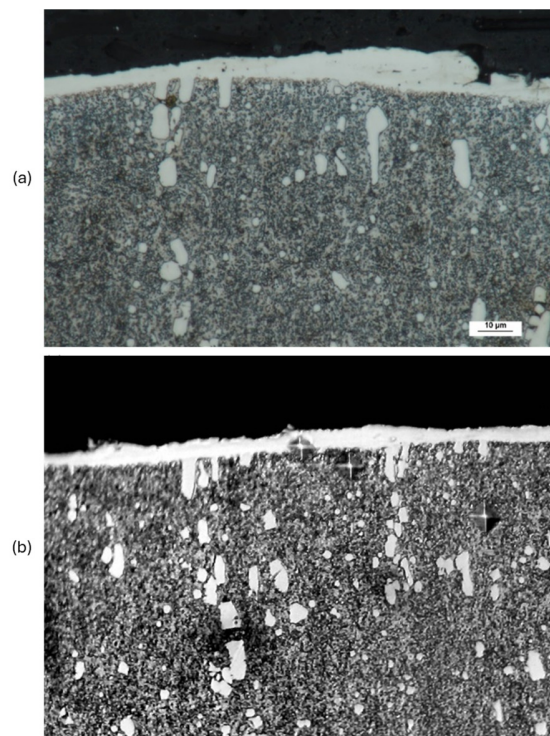


Fig. 8. Cross-sectional SEM images of the white layer: (a) conventional EDM and (b) PMEDM (DF=60%, I_p =15A, Speed=120 mm/min).

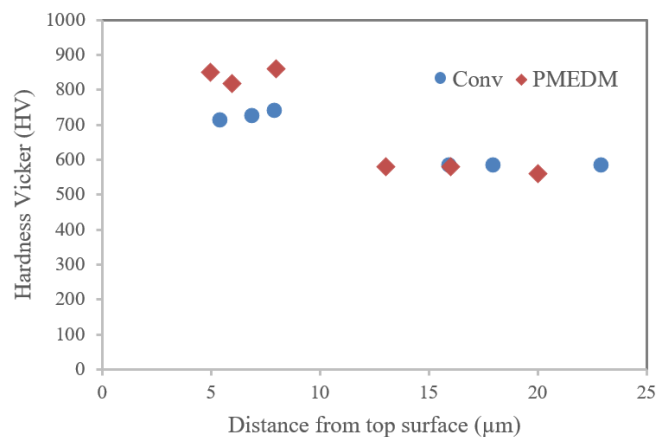


Fig. 9. Microhardness depth profile from the EDMed surface.

In PMEDM: Additional or intensified peaks corresponding to Si and C, confirming transfer and incorporation of SiC particles (or their decomposition products) into the recast layer. This elemental migration contributes to the observed hardness increase and may enhance surface wear resistance through carbide formation.

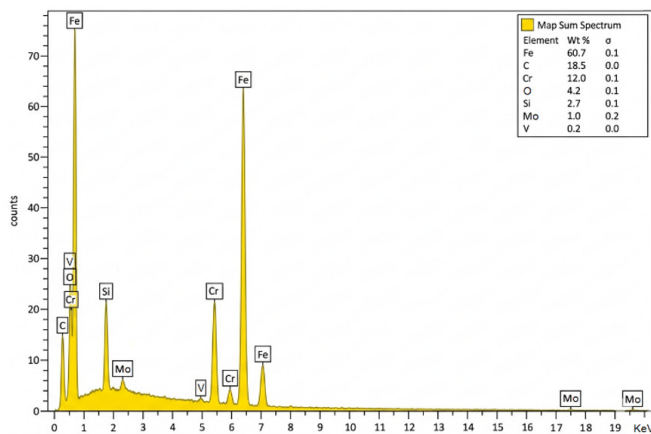


Fig. 10. EDS analysis.

IV. CONCLUSION

This study applied the Taguchi method to systematically investigate the effects of process parameters on Material Removal Rate (MRR) and Surface Roughness (SR) (Ra) during Electrical Discharge Machining (EDM) and Silicon Carbide Powder-Mixed EDM (SiC PMEDM) of SKD11 tool steel. The main findings are:

- The Taguchi approach effectively identified the optimal parameter combinations influencing MRR and Ra. In conventional EDM, the highest MRR was obtained at a Duty Factor (DF) of 75%, a peak current of 24 A, and an electrode speed of 180 mm/min.
- Incorporating SiC powder enhanced process stability and predictability, achieving a higher model accuracy ($R^2 = 91.79\%$), indicating improved consistency in discharge behavior.
- PMEDM increased MRR by 9.51% compared to conventional EDM, demonstrating its effectiveness in improving machining efficiency; however, this was accompanied by a deterioration in SR.
- PMEDM significantly modified surface integrity, increasing white layer thickness by 44.7% and surface microhardness by 18.1%, confirming that SiC particles promote stronger surface hardening and thicker recast layer formation.

Overall, this work demonstrates that SiC-PMEDM can enhance machining efficiency and surface hardness at lower discharge energy levels, while also revealing the significant trade-off between productivity and surface quality. In addition, future work should focus on detailed microstructural and residual stress analysis to improve surface integrity.

DECLARATION OF COMPETING INTERESTS

The authors declare that they have no known competing financial interests or personal relationships that could have appeared to influence the work reported in this paper.

ACKNOWLEDGMENT

The authors gratefully acknowledge the support provided by Thammasat University Research Fund, Contract No.TUFT 99/2567 and Phranakhon Si Ayutthaya Rajabhat University, Faculty of Science and Technology, for the provision of equipment and facilities.

DATA AVAILABILITY

The raw and processed data required to reproduce the reported findings are available from the corresponding author upon reasonable request.

AI USE AND DECLARATION OF GENERATIVE AI USE

During the preparation of this work, the authors used Gemini (Google LLC) specifically to design, structure, and refine the layout of Figure 2 (the systematic experimental research workflow flowchart).

This tool was utilized solely to enhance the visual clarity, structural formatting, and presentation logic of the workflow schematic, ensuring that it aligns with high-level academic publishing standards. The software was not used to synthesize, analyze, or interpret any experimental data, nor did it alter any original scientific data or images.

After generating the schematic layout, the authors thoroughly reviewed, verified, and edited all content to ensure exact alignment with the physical experimental methodology. The authors take full responsibility for the accuracy and integrity of the content of this published article.

REFERENCES

- [1] S. Gudur and V. Potdar, "Effect of silicon carbide powder mixed EDM on machining characteristics of SS 316L material experimentation," *International Journal of Innovative Research in Science, Engineering and Technology*, vol. 4, pp. 8131–8141, Sept. 2015, <https://doi.org/10.15680/IJRSET.2015.0409017>.
- [2] M. A. Razak, A. M. Abdul-Rani, and A. M. Nanimina, "Improving EDM efficiency with silicon carbide powder-mixed dielectric fluid," *International Journal of Materials, Mechanics and Manufacturing*, vol. 3, no. 1, pp. 40–43, 2015.
- [3] T.-H. Tran *et al.*, "Electrical Discharge Machining with SiC Powder-Mixed Dielectric: An Effective Application in the Machining Process of Hardened 90CrSi Steel," *Machines*, vol. 8, no. 3, 2020, Art. no. 36, <https://doi.org/10.3390/machines8030036>.
- [4] V. T. Nguyen, V. T. Dinh, D. P. Phan, D. B. Vu, and N. P. Vu, "Determination of Best Input Factors in Powder-Mixed Electrical Discharge Machining 90CrSi Steel using Multi-Criteria Decision Making Methods," *Engineering, Technology & Applied Science Research*, vol. 15, no. 1, pp. 19121–19127, Feb. 2025, <https://doi.org/10.48084/etasr.9171>.
- [5] T. P. T. Le, V. T. Dinh, T. Q. D. Nguyen, D. B. Vu, and T. T. Vu, "Application of the Multi-Criteria Decision Method to Find the Best Input Factors for Electrical Discharge Machining 90CrSi Tool Steel using Graphite Electrodes," *Engineering, Technology & Applied Science Research*, vol. 14, no. 6, pp. 18883–18888, Dec. 2024, <https://doi.org/10.48084/etasr.9114>.
- [6] S. D. Mohanty, S. S. Mahapatra, and R. C. Mohanty, "PCA based hybrid Taguchi philosophy for optimization of multiple responses in EDM," *Sādhanā*, vol. 44, no. 1, 2019, Art. no. 2, <https://doi.org/10.1007/s12046-018-0982-z>.
- [7] P.-N. Huu, "Study of the effects of process parameters on tool wear rate in powder mixed electrical discharge machining by Taguchi method,"

- VNUHCM *Journal of Science and Technology Development*, vol. 20, no. K7, pp. 55–60, 2017, <https://doi.org/10.32508/stdj.v20iK7.1375>.
- [8] A. Al-Khazraji, S. A. Amin, and S. M. Ali, "The effect of SiC powder mixing electrical discharge machining on white layer thickness, heat flux and fatigue life of AISI D2 die steel," *Engineering Science and Technology, an International Journal*, vol. 19, no. 3, pp. 1400–1415, Sept. 2016, <https://doi.org/10.1016/j.jestch.2016.01.014>.
- [9] M. Manoj and A. Gopal, "Modelling, Investigation of Process Responses, Surface Assessment and Parametric Optimization in Powder Mixed Electrical Discharge Diamond Grinding of Ti6Al4V Utilizing Grey-Based Taguchi Approach," *Transactions of FAMENA*, vol. 44, no. 3, pp. 93–112, 2020, <https://doi.org/10.21278/TOF.44308>.
- [10] K. Ishfaq, M. Asad, S. Anwar, C. I. Pruncu, M. Saleh, and S. Ahmad, "A Comprehensive Analysis of the Effect of Graphene-Based Dielectric for Sustainable Electric Discharge Machining of Ti-6Al-4V," *Materials*, vol. 14, no. 1, 2021, Art. no. 23, <https://doi.org/10.3390/ma14010023>.
- [11] K. Ishfaq, M. Sana, M. A. Mahmood, and S. Anwar, "An energy concisions analytical modelling approach with experimental verification for cutting performance assessment in EDM of Ti-based superalloy," *Physica Scripta*, vol. 99, no. 8, 2024, Art. no. 085996, <https://doi.org/10.1088/1402-4896/ad6409>.
- [12] K. Ishfaq, M. A. Maqsood, S. Anwar, M. Harris, A. Alfaify, and A. W. Zia, "EDM of Ti6Al4V under nano-graphene mixed dielectric: a detailed roughness analysis," *The International Journal of Advanced Manufacturing Technology*, vol. 120, no. 11, pp. 7375–7388, 2022, <https://doi.org/10.1007/s00170-022-09207-y>.
- [13] B. T. Long, N. H. Phan, N. Cuong, and N. D. Toan, "Surface quality analysis of die steels in powder-mixed electrical discharge machining using titan powder in fine machining," *Advances in Mechanical Engineering*, vol. 8, no. 7, 2016, Art. no. 1687814016657732, <https://doi.org/10.1177/1687814016657732>.
- [14] Y.-F. Chen, Y.-J. Lin, Y.-C. Lin, S.-L. Chen, and L.-R. Hsu, "Optimization of electrodischarge machining parameters on ZrO2 ceramic using the Taguchi method," in *Proceedings of the Institution of Mechanical Engineers, Part B: Journal of Engineering Manufacture*, vol. 224, no. 2, pp. 195–205, 2010, <https://doi.org/10.1243/09544054JEM1437>.
- [15] G. Bhadauria, S. K. Jha, B. N. Roy, and N. S. Dhakry, "Electrical-Discharge Machining of Tungsten Carbide (WC) and its composites (WC-Co) – A Review," *Materials Today: Proceedings*, vol. 5, no. 11, Part 3, pp. 24760–24769, 2018, <https://doi.org/10.1016/j.matpr.2018.10.274>.
- [16] H.-M. Chow, L.-D. Yang, C.-T. Lin, and Y.-F. Chen, "The use of SiC powder in water as dielectric for micro-slit EDM machining," *Journal of Materials Processing Technology*, vol. 195, no. 1–3, pp. 160–170, Jan. 2008, <https://doi.org/10.1016/j.jmatprotec.2007.04.130>.
- [17] A. Kadirvel, P. Hariharan, and S. Gowri, "Experimental Investigation on the Electrode Specific Performance in Micro-EDM of Die-Steel," *Materials and Manufacturing Processes*, vol. 28, no. 4, pp. 390–396, 2013, <https://doi.org/10.1080/10426914.2013.763959>.
- [18] S. Ramesh and M. Jenarathanan, "Optimizing the powder mixed EDM process of nickel based super alloy," in *Proceedings of the Institution of Mechanical Engineers, Part E: Journal of Process Mechanical Engineering*, vol. 235, no. 4, pp. 1092–1103, 2021, <https://doi.org/10.1177/09544089211002782>.
- [19] P. Nakwong and A. Muttamara, "Taguchi Optimization of MRR in Magnesium AZ91 Using EDM with Graphite Electrode," *Key Engineering Materials*, vol. 1014, pp. 11–16, 2025, <https://doi.org/10.4028/p-1kPPWg>.
- [20] F. Rajabinasab, V. Abedini, M. Hadad, and R. Hajjghorbani, "Experimental investigation of the effect of tool material on the performance of AISI 4140 steel in the rotary near dry electrical discharge machining," in *Proceedings of the Institution of Mechanical Engineers, Part E: Journal of Process Mechanical Engineering*, vol. 234, no. 4, pp. 308–317, 2020, <https://doi.org/10.1177/0954408920922102>.
- [21] E. Garba *et al.*, "A Review of Electrode Manufacturing Methods for Electrical Discharge Machining: Current Status and Future Perspectives for Surface Alloying," *Machines*, vol. 11, no. 9, Sept. 2023, Art. no. 906, <https://doi.org/10.3390/machines11090906>.
- [22] P. N. Jayantibhai and B. Khatri, "A Comprehensive Investigation into the Material Removal Capability of Powder Mixed Wire Electric Discharge Machining," *Tuijin Jishu/Journal of Propulsion Technology*, vol. 44, no. 3, 2023.
- [23] S. A. Khan, M. Omer, M. U. Farooq, S. Anwar, and A. A. Adediran, "Effect of powder particle concentration, pulse duration, and pulse current on machined surface characterization produced via EDM of biocompatible WE-43Mg alloy," *Scientific Reports*, vol. 15, no. 1, 2025, Art. no. 33927, <https://doi.org/10.1038/s41598-025-10123-w>.
- [24] V. Le, T. Banh, X. Tran, and T. H. M. Nguyen, "Improving Surface Roughness by Electrical Discharge Machining with Tungsten Powder" *ASEAN Engineering Journal*, vol. 9, no. 1, 2019, <https://doi.org/10.11113/aej.v9.15507>.
- [25] S. Srivastava, M. Vishnoi, M. T. Gangadhar, and V. Kukshal, "An insight on Powder Mixed Electric Discharge Machining: A state of the art review," in *Proceedings of the Institution of Mechanical Engineers, Part B: Journal of Engineering Manufacture*, vol. 237, no. 5, pp. 657–690, 2022, <https://doi.org/10.1177/09544054221111896>.
- [26] A. Abdudeen, J. E. Abu Qudeiri, A. Kareem, T. Ahammed, and A. Ziout, "Recent Advances and Perceptive Insights into Powder-Mixed Dielectric Fluid of EDM," *Micromachines*, vol. 11, no. 8, 2020, Art. no. 754, <https://doi.org/10.3390/mi11080754>.
- [27] G. Talla, S. Gangopadhyay, and C. Biswas, "State of the art in powder-mixed electric discharge machining: A review," in *Proceedings of the Institution of Mechanical Engineers, Part B: Journal of Engineering Manufacture*, vol. 231, no. 14, pp. 2511–2526, 2016, <https://doi.org/10.1177/0954405416634265>.
- [28] V. T. Le, T. L. Banh, X. T. Tran, and N. T. H. Minh, "Surface Modification Process by Electrical Discharge Machining with Tungsten Carbide Powder Mixing in Kerosene Fluid," *Applied Mechanics and Materials*, vol. 889, pp. 115–122, 2019, <https://doi.org/10.4028/www.scientific.net/AMM.889.115>.
- [29] S. K. Sahu and S. Datta, "Experimental studies on graphite powder-mixed electro-discharge machining of Inconel 718 super alloys: Comparison with conventional electro-discharge machining," in *Proceedings of the Institution of Mechanical Engineers, Part E: Journal of Process Mechanical Engineering*, vol. 233, no. 2, pp. 384–402, 2018, <https://doi.org/10.1177/0954408918787104>.